JOURNAL OF SOLID STATE CHEMISTRY 31, 81–93 (1980)

Thermal Decomposition of Manganese Oxyhydroxide

J. A. LEE,* C. E. NEWNHAM,* F. S. STONE,† AND F. L. TYE*

**Berec Group Ltd., Group Technical Centre, St. Ann's Road, London N15 3TJ*; †*School of Chemistry, University of Bath, Claverton Down, Bath BA2 7AY, England*

Received August 31, 1978; in final form February 28, 1979

Temperature-programmed thermal decomposition of γ- and α-manganese oxyhydroxide has been studied between 20 and 670°C under vacuum and under a low pressure (10 Torr) of oxygen. Solid products at various temperatures have been analyzed by X-ray diffractometry. Under vacuum γ-MnOOH decomposed below 400°C to a mixture of Mn_5O_8, α-Mn_3O_4, and water according to the reaction scheme: $8MnOOH \rightarrow Mn_5O_8 + Mn_3O_4 + 4H_2O$. Above this temperature Mn_5O_8 was converted to α-Mn_3O_4 as a result of oxygen removal. The vacuum dehydration at 250°C of oxyhydroxide rich in α-MnOOH led to the formation of a new modification of Mn_2O_3 isostructural with corundum (α-Al_2O_3). In oxygen both oxyhydroxides decomposed to β-MnO_2. γ-MnOOH transformed directly to β-MnO_2 while α-MnOOH appeared to transform via corundum-phase Mn_2O_3 as an intermediate.

Introduction

The thermal behavior of synthetic γ-MnOOH was first reported by Dubois (*1*), who stated that using a linear heating program the solid decomposed at 250°C under vacuum to give a variety of Mn_2O_3 which later became designated as γ-Mn_2O_3. Verwey and de Boer (*2*) confirmed this work and suggested that the structure of this modification of Mn_2O_3 could be described as a spinel (Mn_3O_4) containing cation vacancies ($Mn_{2.66}\square_{0.34}O_4$).

The subject was later taken up by Feitknecht and his school (*3*), and it was established by Brunner (4) that both synthetic and natural γ-MnOOH when heated isothermally at 400°C in an environment of low oxygen pressure decomposed topotactically to an oxide of ideal composition $MnO_{1.6}$. Oswald *et al.* (*5*) confirmed the phase to be Mn_5O_8 and a detailed structural analysis of this oxide was subsequently published by Oswald and Wampetich (*6*).

Sato *et al.* (*7*) recently investigated γ-MnOOH decomposition in an inert atmosphere (N_2) up to 640°C and obtained the *C*-structure sesquioxide α-Mn_2O_3. They suggested it was formed via an intermediate of formula $MnO_{1.63}$, but this product was not identified.

When studied by thermogravimetry, decomposition of γ-MnOOH in an oxygen environment is generally held to produce β-MnO_2. However, close scrutiny of the data presented by Dubois (*1*) and by Sato *et al.* (*7*) indicates that this is not the straightforward oxidation process expected from the reaction

$$4MnOOH + O_2 \rightarrow 4MnO_2 + 2H_2O, \quad (1)$$

but that decomposition may proceed via an intermediate. Sato *et al.* (*7*) concluded that the thermal transformation in oxygen took place via Mn_2O_3 although no evidence was

0022-4596/80/010081-13$02.00/0

presented to confirm the formation of a sesquioxide structure.

In view of the uncertainty which exists regarding the decomposition of γ-MnOOH under vacuum and in oxygen, a reinvestigation of the thermal behavior of γ-MnOOH has been undertaken. The work has been supplemented by an examination of the thermal decomposition of α-MnOOH since this has proved useful in interpreting the behavior of the γ modification.

Experimental

Materials

The preparation of γ-MnOOH (samples A and B) was based on a method described by Giovanoli and Leuenberger (*8*). Sample A was prepared by the addition of aqueous ammonia (150 cm^3, 0.2 *M*) to a stirred solution of manganous sulfate (5.07 g, 500 cm^3 H_2O) containing hydrogen peroxide (10.2 cm^3, 30% w/v) at room temperature. A chocolate-brown precipitate formed instantaneously and this was heated in the aqueous solution to 100°C and refluxed for 26 hr. The resulting yellow-brown solid was filtered off and air-dried at 100°C for 12 hr. Chemical analysis showed a mean oxidation state of 3.02 for the manganese corresponding to $x = 1.51$ in formula "MnO_x" conventionally used to describe these systems. Sample B was prepared in a similar manner except that precipitation was carried out at 5°C and the product filtered off, washed thoroughly with distilled water, and dried under vacuum overnight at ambient temperature. Chemical analysis showed a sample composition of $MnO_{1.52}$.

The preparation of α-MnOOH was also based on a procedure reported by Giovanoli and Leuenberger (*8*). Well-crystallized γ-MnO_2 (2.0 g) prepared by the disproportionation of α-Mn_3O_4 in hot dilute nitric acid was heated in a round-bottomed flask at 90°C together with cinnamyl alcohol (2.4 g) and xylene (40 cm^3) for 6 days. The product was filtered off, washed thoroughly with industrial methylated spirits, and air-dried at 25°C. Interplanar distances taken from an X-ray diffractometer trace are compared with those of natural α-MnOOH (groutite) (*9*) in Table I. All the peaks in the pattern can be indexed on the basis of α-MnOOH although some of the weaker lines reported for natural groutite could not be measured. Chemical analysis indicated a composition corresponding to $MnO_{1.45}$.

A sample of Mn_5O_8 was kindly supplied by Dr. R. Giovanoli of the University of Berne. It had been prepared by the controlled oxidation of finely divided MnO obtained from the decomposition of Mn(II) oxalate in hydrogen.

TABLE I

X-RAY DIFFRACTION DATA FOR SYNTHETIC AND NATURAL GROUTITE (α-MnOOH)

Synthetic α-MnOOH			Natural α-MnOOH		
d (Å)	*I*/*I*°	*hkl*	*d* (Å)	*I*/*I*°	*hkl*
			5.34	20	020
4.19	100	110	4.20	100	110
			3.47	20	120
2.86	35	130	2.81	70	130
2.63	85	040	2.67	70	040
2.54	50	021	2.54	5	021
			2.42	5	101
2.39	80	111	2.38	40	111
2.31	55	140	2.30	60	140
			2.28	5	200
2.22	35	210	2.22	10	210
			2.10	5	220
			2.01	5	131
			1.91	20	041 150
			1.781	5	060
			1.762	10	211
			1.737	40	240
1.694	90	221	1.695	50	221
1.62	25	151	1.608	40	151
			1.561	30	250
1.514	25	061	1.515	30	061
			1.487	5	
			1.463	30	
			1.449	40	

Methods

The TG/DTG apparatus was based on a Cahn microbalance and has been described previously (*10*). Decompositions under dynamic vacuum were carried out by evacuating the sample at room temperature to a pressure of $5–7\times10^{-5}$ Torr and then applying a linear heating program of 5°C min^{-1}. Decompositions in oxygen were carried out by evacuating the sample as above and then admitting oxygen at 10 Torr. Thermogravimetry in this case was performed in the closed system: The heating rate was again 5°C min^{-1}.

Compositions of the manganese oxides/hydroxides are conveniently expressed in the form MnO_x where x is related to the mean oxidation state of Mn and ranges from 1.0 for MnO to 2.0 for MnO_2; $MnO_{1.50}$ thus describes both Mn_2O_3 and MnOOH.

The procedure for chemical analysis of the oxyhydroxides and their decomposition products was based on methods employed by Vetter and Jaeger (*11*) and Freeman and Chapman (*12*). The sample, typically 60 mg, was refluxed in iron-stabilized sodium oxalate solution (10 cm^3, 0.02 *M*) containing sulfuric acid (2 cm^3, 20% v/v) for 30 min. This solution was diluted to 25 cm^3, heated to 80°C, and titrated with 0.02 *M* $KMnO_4$ (V_1). To the same solution was added sodium pyrophosphate (~4 g) which dissolved. The pH was adjusted to 6.5–7.0 by addition of sodium hydroxide pellets and the solution was titrated potentiometrically with 0.02 *M* $KMnO_4$ (V_2). Finally, the volume of $KMnO_4$ required to standardize 10 cm^3 of sodium oxalate solution was noted (V_0). The value of x in MnO_x was calculated from the relationship

$$x = 1+5[(V_0-V_1)/(8V_2-2V_1)].$$

Results and Discussion

(*a*) *Thermogravimetry under Vacuum*

The thermal analysis of γ-MnOOH (sample A) under vacuum is illustrated in Fig. 1. The rate of weight loss shows two peaks between room temperature and 700°C. The aggregated weight loss of 10.7% associated with the first decomposition step (Fig.1, broken curve) is in good agreement with the expected water removal resulting from the dehydroxylation of γ-MnOOH to Mn_2O_3 (10.2%):

$$2MnOOH \rightarrow Mn_2O_3+H_2O. \quad (2)$$

In order to characterize the dehydroxylation product an X-ray diffraction trace was recorded of the product obtained at the end of the first decomposition step (370°C) which is shown in Fig. 2b. The trace did not correspond to the patterns for γ-Mn_2O_3 reported by Dubois (*1*), Verwey and de Boer (*2*), and other workers (*13, 14*) (Fig. 3), and it did not resemble that of the common form of manganese sesquioxide, α-Mn_2O_3. Close examination of the X-ray data revealed that about half of the lines could be attributed to the spinel α–Mn_3O_4, the diffractometer trace of which is shown in Fig. 2c. This suggests a mixture of two products, one of which is α-Mn_3O_4.

Chemical analysis of γ-MnOOH (sample A) and its dehydroxylation product showed that neither oxidation nor reduction had occurred upon heat treatment, x in MnO_x being equal to 1.51 and 1.50 before and after decomposition, respectively. As α-Mn_3O_4 can be written as $MnO_{1.33}$ the other component must possess an x value intermediate between 1.50 and 2.00. The only well-characterized oxide of manganese possessing a mean oxidation state between 3 and 4 is Mn_5O_8. An X-ray diffractometer trace of this oxide is shown in Fig. 4 and it is evident that the remainder of the lines in Fig. 2b correspond with this oxide.

Bearing in mind the earlier results, we note that the formation of α-Mn_3O_4 and Mn_5O_8 can be hypothetically seen as arising from the decomposition of an intermediate conveniently represented by the

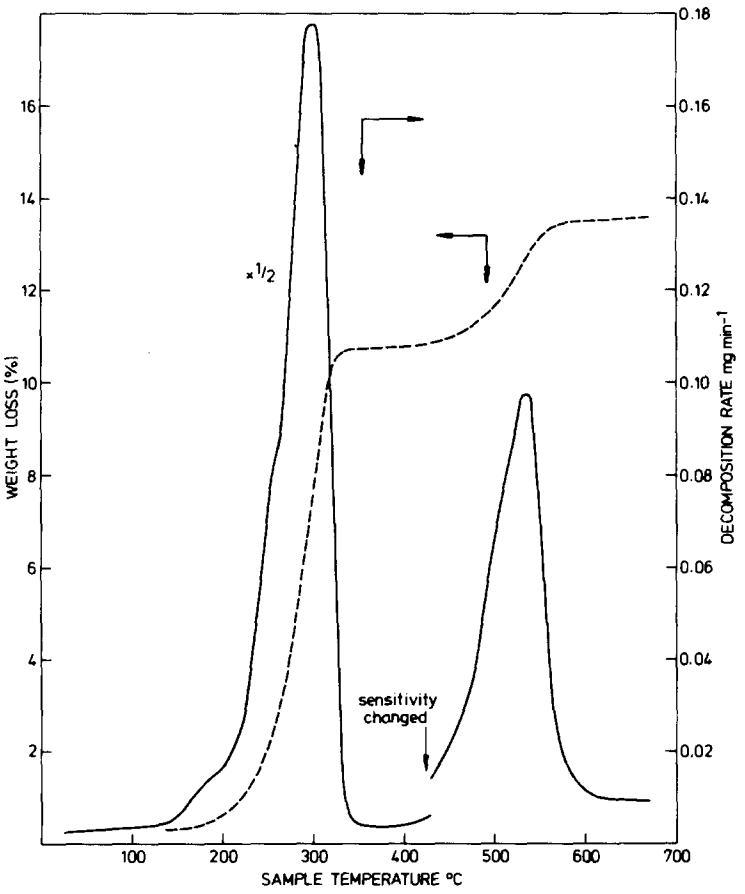

FIG. 1. Thermal decomposition under vacuum of γ-MnOOH (sample A): Weight loss (– – –) and rate of decomposition (——) curves.

formula Mn_2O_3:

$$4Mn_2O_3 \rightarrow Mn_3O_4 + Mn_5O_8, \quad (3)$$

the overall reaction from the oxyhydroxide being described by

$$8MnOOH \rightarrow Mn_3O_4 + Mn_5O_8 + 4H_2O. \quad (4)$$

The decomposition under dynamic vacuum to equimolar amounts of Mn_3O_4 and Mn_5O_8 is thus consistent with weight loss, X-ray diffraction, and chemical analysis data and has not hitherto been reported. The process may have been undetected by other workers because of the relatively weak X-ray diffraction pattern of Mn_5O_8 compared with that of α-Mn_3O_4. X-Ray analysis at low sensitivity would reveal only the presence of α-Mn_3O_4 and as the analytical composition of the dehydroxylated product corresponds to a mean valency state of 3 for the manganese this could have given rise to the claims for a modification of Mn_2O_3 possessing an X-ray pattern almost identical to that of α-Mn_3O_4, i.e., γ-Mn_2O_3.

At a higher temperature the Mn_5O_8 component of the mixture decomposes to Mn_3O_4:

$$3Mn_5O_8 \rightarrow 5Mn_3O_4 + 2O_2. \quad (5)$$

The expected weight loss of 3.0% for such a process is in good agreement with the figure

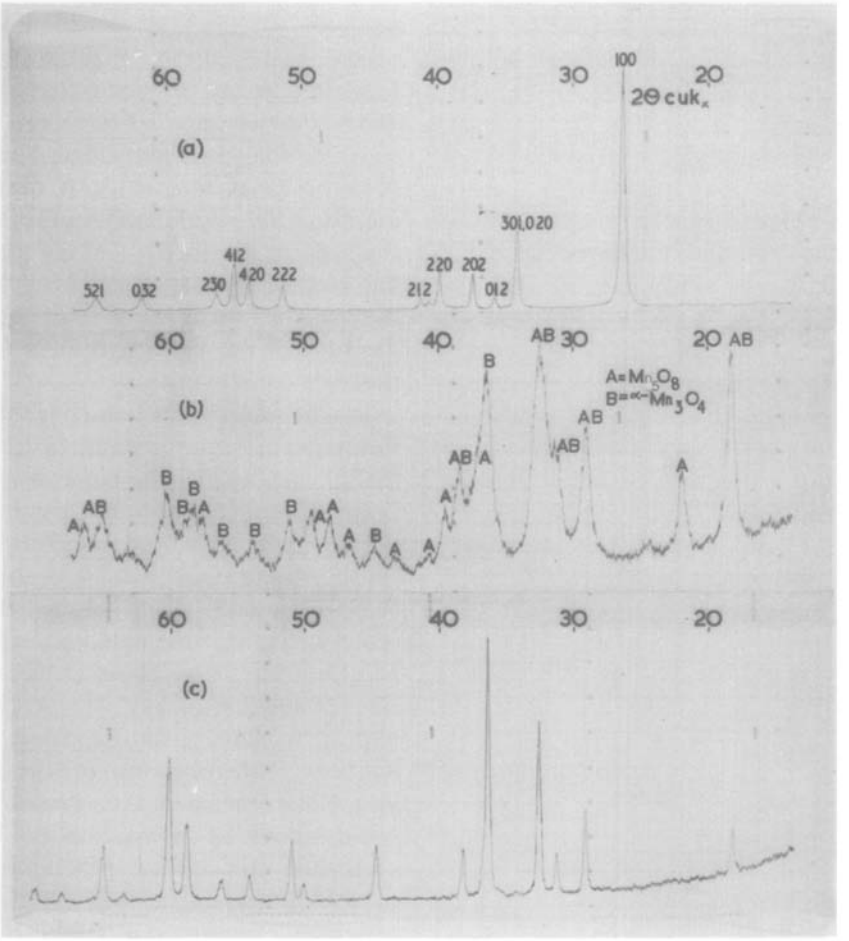

FIG. 2. X-Ray diffractometer traces (Cu$K\alpha$) of the products obtained by application of a linear heating program (5°C min^{-1}) to γ-MnOOH (sample A) under vacuum. These correspond to temperatures of (a) 25, (b) 370, and (c) 670°C on the thermal analysis curve in Fig. 1.

of 2.8% found experimentally at ~500°C and shown in Fig. 1. An X-ray diffractometer trace of the decomposition product at 670°C (Fig. 2c) confirmed the presence of solely α-Mn_3O_4. There are no data in the literature concerning the thermal behavior of Mn_5O_8 under vacuum. In air or oxygen, however, Oswald *et al.* (*5*) found that at 550°C there was decomposition to α-Mn_2O_3. Recent work by Agopsowicz *et al.* (*15*) indicates that this path may also be followed in an argon environment. Our results show that this does not happen under dynamic vacuum.

The thermal analysis curve under vacuum of the oxyhydroxide precipitated at 5°C (sample B) is illustrated in Fig. 5. Whereas only two decomposition steps were observed for sample A, sample B decomposed in *three* distinct stages. The weight loss of 11.2% associated with the initial step was close to that expected for a compositional change from MnOOH to Mn_2O_3, i.e., 10.2%. Chemical analysis of the dehydroxylation product after heating to 350°C gave a value for x in MnO_x of 1.50; this confirmed that as for sample A no change in the mean

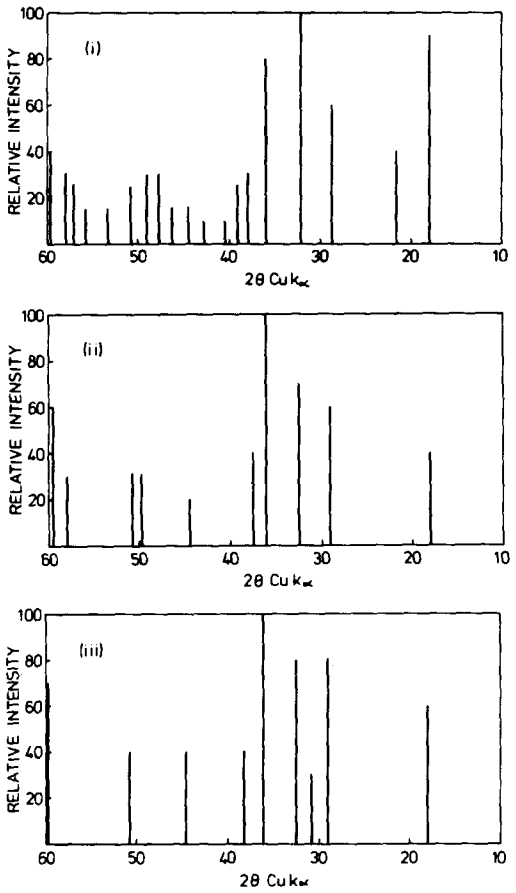

FIG. 3. X-Ray line diagrams for (i) γ-MnOOH (sample A) dehydroxylated under vacuum, (ii) γ-Mn_2O_3 prepared by Moore *et al.* (*13*) and (iii) γ-Mn_2O_3 prepared by Drotschmann (*14*).

oxidation state of the manganese ions had taken place upon thermal treatment. However, it can be seen from the X-ray diffractometer trace in Fig. 6b that the structure of the product differed from that obtained using sample A. A most striking feature is the small number of lines, and yet the pattern could not be ascribed to any known oxide of manganese. It appeared that the product could correspond only to Mn_2O_3, but the X-ray pattern differed from that of γ- or α-Mn_2O_3.

In the course of studying the transformation of natural groutite (α-MnOOH) at 300°C into β-MnO_2, Lima-de-Faria and Lopes-Vieira (*16*) observed some weak and diffuse spots on X-ray oscillation photographs which could not be ascribed to β-MnO_2. They noted that some of these spots fitted well with what could be expected for Mn_2O_3 with a corundum structure having $a = 4.9$ and $c = 14.3$ Å. The results do not appear to have been repeated by other workers, but following this lead careful inspection showed that the pattern in Fig. 6b could indeed be indexed on the basis of a corundum unit cell using the literature data for α-Al_2O_3 (*17*) and α-Fe_2O_3 (*18*) and the assignment presented in Table II. The unit-cell parameters have been calculated by means of the usual relationship for

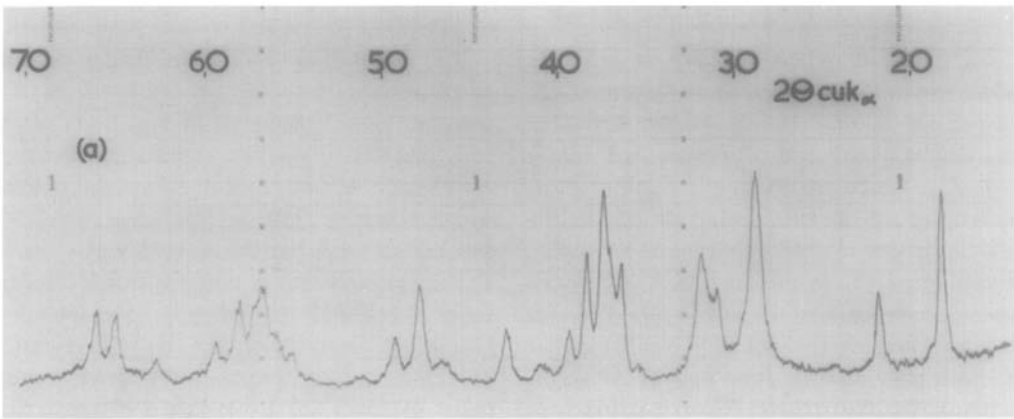

FIG. 4. X-Ray diffractometer trace (Cu*Kα*) of Mn_5O_8.

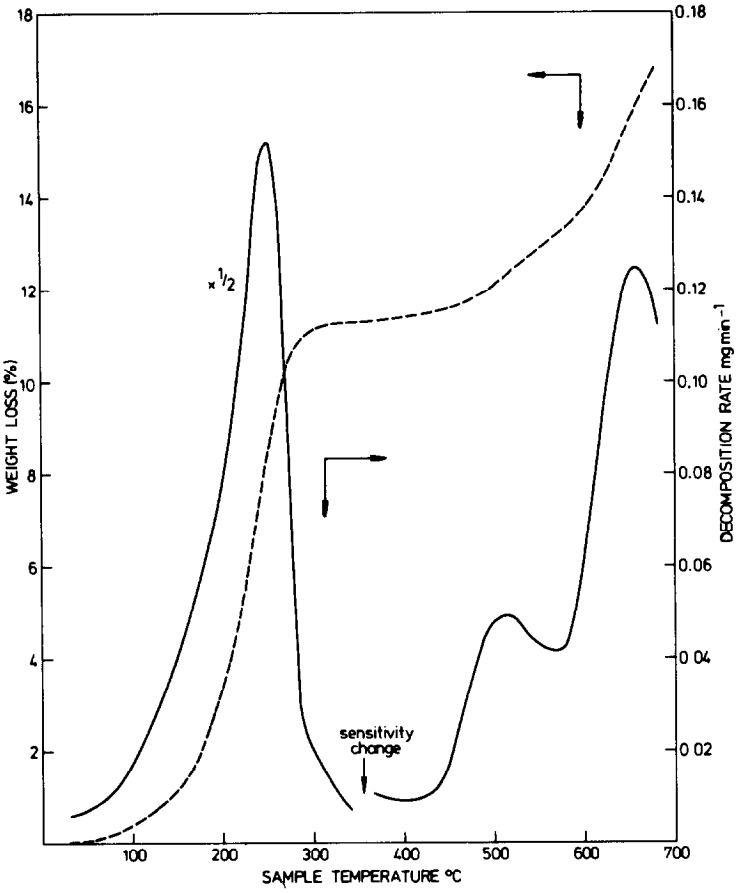

FIG. 5. Thermal decomposition under vacuum of MnOOH (sample B): Weight loss (– – –) and rate of decomposition (——) curves.

hexagonal unit cells (*19*):

$$\frac{1}{d_{hkl}^2}=\frac{4}{3}\frac{(h^2+hk+k^2)}{a^2}+\frac{l^2}{c^2}. \qquad (6)$$

The results obtained were $a = 5.04$ and $c = 14.12$ Å, respectively, in good agreement with the approximate values proposed by Lima-de-Faria and Lopes-Vieira (*16*). That these lattice parameters are of the magnitude to be expected for manganese sesquioxide possessing a corundum structure may be seen by comparison of the hexagonal unit-cell volumes of other sesquioxides existing in the corundum phase with that calculated for Mn_2O_3. This relationship is illustrated graphically in Fig. 7.

In order to understand why the dehydroxylation products from the two preparations of γ-MnOOH differed, the X-ray diffractograms of samples A and B were examined closely. These are shown in Figs. 2a and 6a, respectively. The interplanar distances for sample A are in good agreement with those given in the literature for natural γ-MnOOH (manganite) (*20*). The pattern of sample B, while strongly resembling that of γ-MnOOH, is less intense and the peaks are broader than those of sample A. These differences alone could be explained by the smaller particle size. However, a peak is present at $2\theta = 21.0°$ (CuK_α) which cannot be ascribed to γ-MnOOH and there is evidence of splitting of certain other peaks.

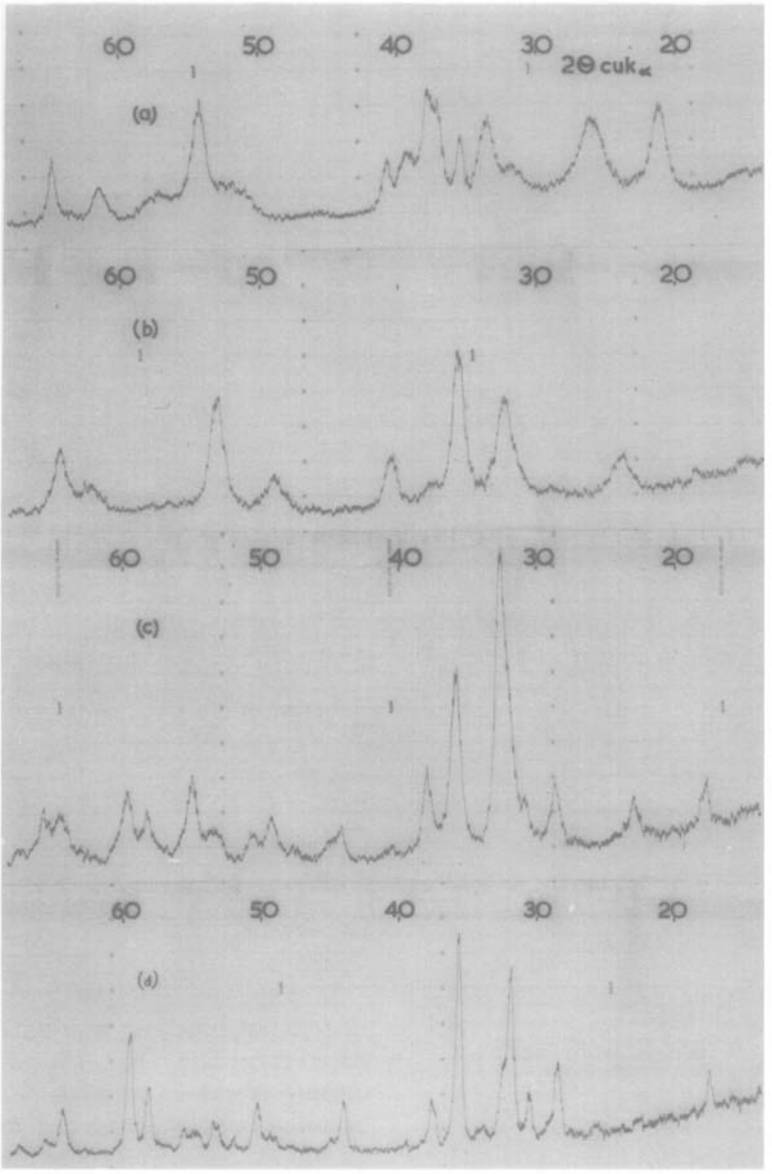

FIG. 6. X-Ray diffractometer traces (CU$K\alpha$) of the products obtained by application of a linear heating program (5°C min^{-1}) to sample B under vacuum. These correspond to temperatures of (a) 25, (b) 350, (c) 565, and (d) 670°C on the thermal analysis curve in Fig. 5.

There is reference in the literature to anomalies between natural γ-MnOOH and synthetic γ-MnOOH. Thus, Feitknecht and Marti (*3*) observed that X-ray patterns of γ-MnOOH samples obtained by precipitation differed slightly from patterns of natural manganite. A new weak line at low diffraction angles appeared and some weak lines expected at larger angles of diffraction were missing. Gattow (*21*) reports that the oxidation of an alkaline manganous sulfate solution with hydrogen peroxide produces

TABLE II

X-RAY DIFFRACTION DATA FOR Mn_2O_3: CORUNDUM STRUCTURE

hkl	2θ	D_{obs}	D_{calc}	$(I_{hkl}/I_{110})\times 100$
012	23.7	3.75	3.71	30
104	32.3	2.77	2.75	65
110	35.6	2.52	2.52	100
113	40.6	2.22	2.22	35
024	48.9	1.86	1.86	25
116	53.2	1.72	1.72	75
124	62.2	1.49	1.49	15
030 or 300	64.2	1.45	1.45	45

oxyhydroxide with a rather diffuse X-ray pattern slightly displaced from the X-ray pattern of natural γ-MnOOH. Moreover, he refers to a new strong line appearing at $2\theta = 22.0°$. This is close to the extra line in the pattern of sample B. Gattow concluded that it was necessary to formulate the existence of a compound γ'-MnOOH, but a more likely explanation is that γ'-MnOOH is made up of a mixture of γ-MnOOH and α-MnOOH. The X-ray pattern of the latter is shown in Fig. 8. It can be seen that the extra features

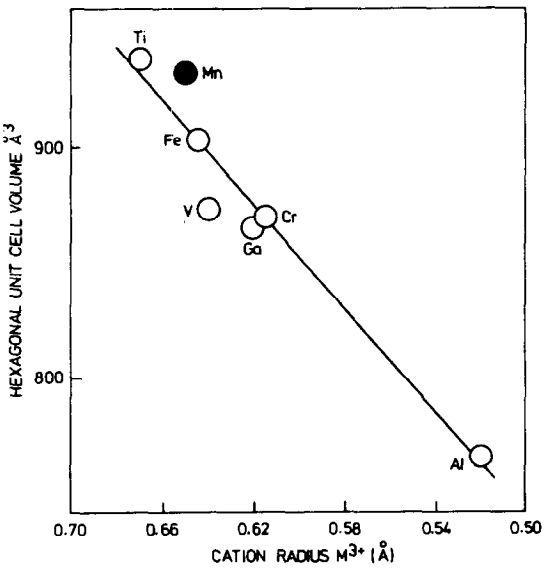

FIG. 7. Hexagonal unit volume as a function of cation radius for sesquioxides of formula $M_2^{3+}O_3$ existing in the corundum phase.

present in the diagram of sample B correspond with peaks in the pattern of α-MnOOH. Confirmation that sample B consisted of a mixture of two oxyhydroxides was obtained by analysis of the decomposition products in nitric acid. Giovanoli and Leuenberger (*8*) have established that γ-MnOOH decomposes in hot dilute nitric acid to β-MnO_2 while α-MnOOH decomposes to γ-MnO_2. These two dioxides may be differentiated from each other by means of their X-ray diffraction patterns. Application of this test to samples A and B produced β-MnO_2 from sample A and a mixture of β- and γ-MnO_2 from sample B, confirming that sample B comprised a mixture of γ- and α-MnOOH.

In view of the above findings the thermal analysis curves of samples A and B would be expected to differ. The formation of the corundum form of Mn_2O_3 almost certainly results from the dehydration of the α-MnOOH component of sample B. α-FeOOH and α-AlOOH, both of which are isostructural with α-MnOOH, dehydrate to give α-Fe_2O_3 and α-Al_2O_3, respectively, both of which possess the corundum structure. Thus there is a close analogy. The decomposition of the corundum form of Mn_2O_3 (which cannot be called α-Mn_2O_3 since this label has been pre-empted for the *C*-structure form!) has not yet been fully investigated. However, examination of X-ray diffraction traces of the products formed beyond the first decomposition stage throws some light on its subsequent fate.

The temperature at which the second decomposition stage occurred for sample B (i.e., 515°C) correspond very closely to that observed for sample A (i.e., 525°C) although the weight loss was much smaller for sample B. As the breakdown of Mn_5O_8 has been shown to be responsible for the second peak in the DTG curve of sample A it is probable that this is the origin of the weight loss found for sample B. This assignment is strongly supported by the following consideration.

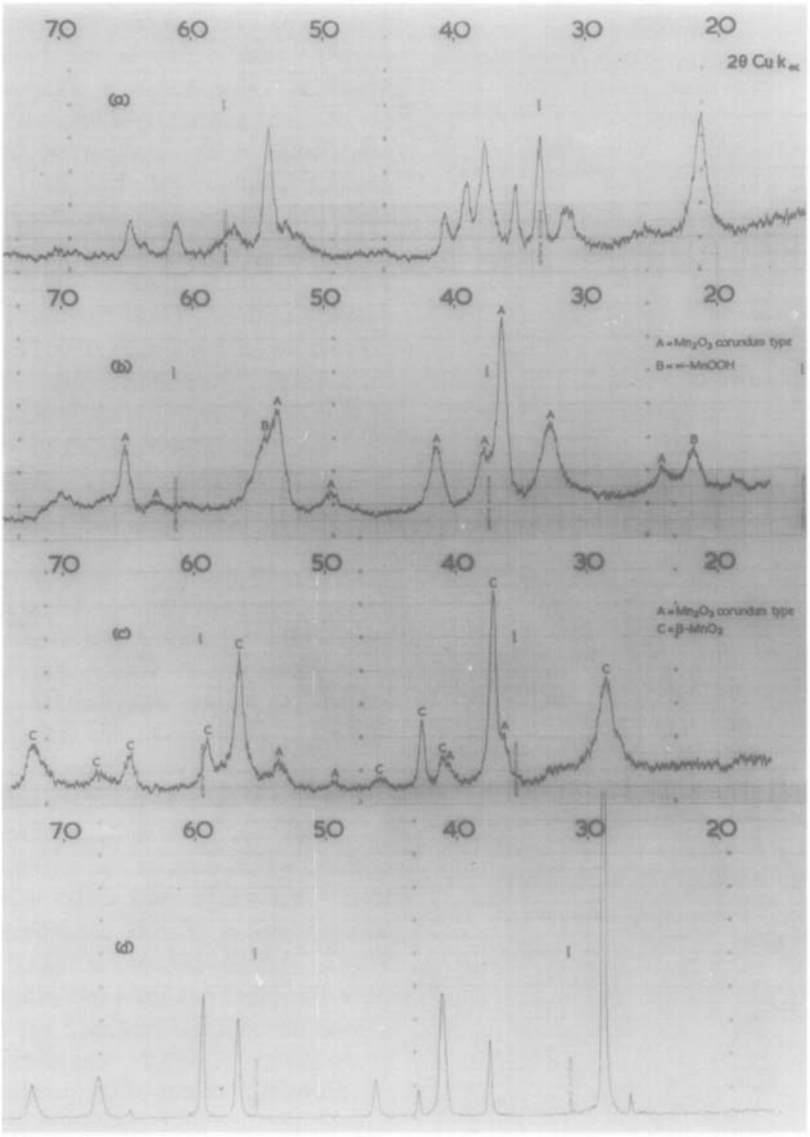

FIG 8. X-Ray diffractometer traces (Cu$K\alpha$) of the products obtained by application of a linear heating program (5°C min^{-1}) to synthetic α-MnOOH in oxygen (10 Torr). These correspond to temperatures of (a) 25, (b) 250, and (c) 350°C on the thermal analysis curve in Fig. 10. Trace (d) is naturally occurring β-MnO_2.

Although corundum Mn_2O_3 was the only phase detected by X-ray diffractometry on completion of the first stage in the vacuum decomposition of sample B, it should be recalled that sample B did originally contain a small proportion of γ-MnOOH and that this will be converted to Mn_5O_8 (plus α-Mn_3O_4) upon vacuum decomposition.

X-ray analysis of the product formed midway between the second and third weight loss peaks for sample B (Fig. 6c) indicated that the corundum phase had disappeared

almost completely (note especially the reduction in the peaks at $2\theta = 40.6$ and 53.2°). However, peaks corresponding specifically to *C*-type Mn_2O_3 (e.g., $2\theta = 23.0$ and 55.0°) and α-Mn_3O_4 could be identified. Thus it appears that between 350 and 565°C the corundum form of Mn_2O_3 undergoes a phase transition to the more stable α modification. The presence of α-Mn_3O_4 can be accounted for by the decomposition of Mn_5O_8 and as one of the initial products from the breakdown of γ-MnOOH.

X-Ray analysis of the product present on termination of the heating program at 670°C (Fig. 6d) revealed predominantly α-Mn_3O_4 with a small amount of α-Mn_2O_3. It is tempting to suggest that the α-Mn_2O_3 breaks down to α-Mn_3O_4, but the total weight loss of 17% recorded for sample B is considerably in excess of the calculated weight loss of 13.3% expected for the compositional change of MnOOH to Mn_3O_4 and of 13.5% found experimentally for sample A. There is therefore a distinct possibility that under the vacuum conditions in which the experiments were conducted Mn_2O_3 goes directly to MnO. This explanation must be considered as tentative às chemical analysis and X-ray diffractometry of the final product removed into air from the balance chamber did not

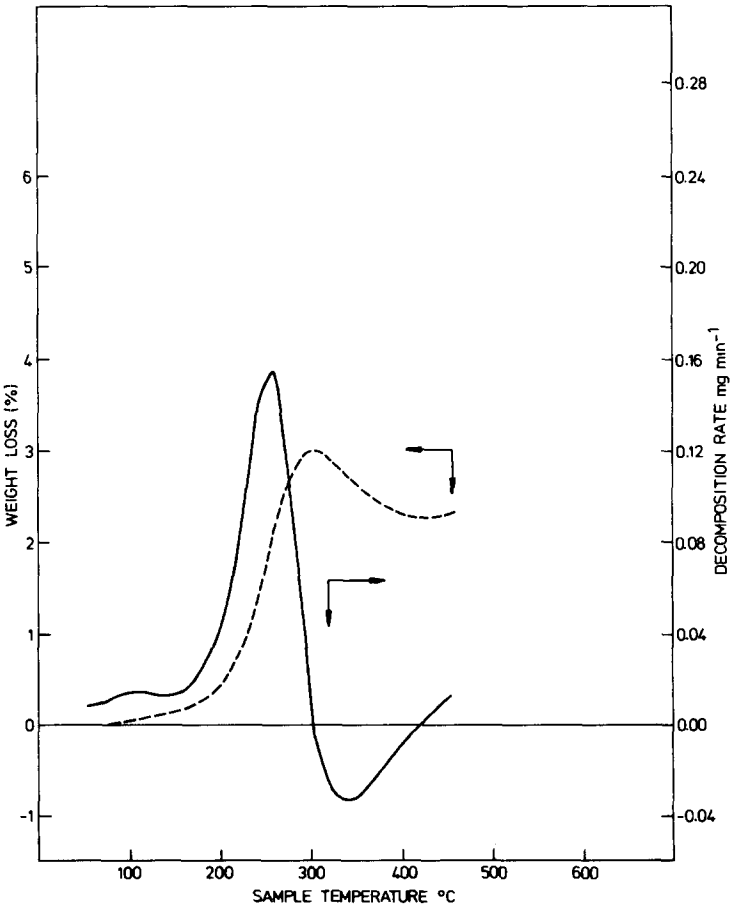

FIG. 9. Thermal decomposition of γ-MnOOH (sample A) in oxygen (10 Torr): Weight loss (– – –) and rate of decomposition (——) curves.

reveal the presence of MnO. However, this can be accounted for by the fact that MnO is probably easily oxidized.

(b) Thermogravimetry in Oxygen

The thermal analysis curve of γ-MnOOH (sample A) under 10-Torr pressure of oxygen is illustrated in Fig. 9. A weight loss in the region of 250°C was followed by a process involving uptake of oxygen. An X-ray diffractometer trace of the product obtained on completion of the absorption step showed this to be β-MnO_2 in accordance with the expected decomposition path given in Eq. (1). X-Ray analysis after termination of programmed runs at selected temperatures prior to this point revealed no phases other than those of γ-MnOOH and β-MnO_2. We conclude that up to 250°C the oxyhydroxide releases water molecules rather more rapidly than it gains oxygen from the gas phase. There is an anion deficit accommodated by anion vacancies in this temperature range and the only new phase is oxygen-deficient

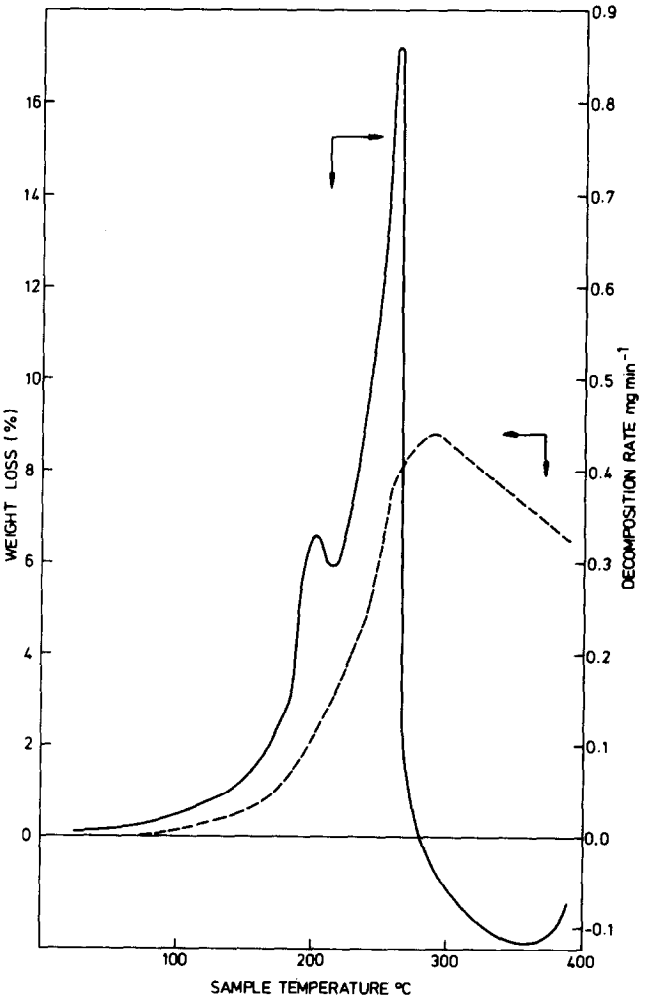

FIG. 10. Thermal decomposition of α-MnOOH in oxygen (10 Torr): Weight loss (– – –) and rate of decomposition (——) curves.

β-MnO_2. Above 250°C the oxygen balance is restored by oxygen uptake.

Sato and co-workers (*7*) suggested that the transformation from γ-MnOOH to β-MnO_2 proceeded via Mn_2O_3, although their findings were inconclusive. From the mode of preparation employed by Sato *et al.* it is likely that their γ-MnOOH sample contained a proportion of α-MnOOH, possibly with a composition intermediate between samples A and B investigated in this study. A specimen of α-MnOOH was therefore synthesized and its thermal behavior investigated. Figure 10 shows the thermal analysis curve of α-MnOOH under 10-Torr pressure of oxygen. It is immediately apparent that the release of water molecules (loss in weight) is more rapid than with γ-MnOOH (sample A, Fig. 9). *Extensive* weight loss has occurred by 250°C. Termination of a programmed run prior to the absorption process and examination of the solid by X-ray analysis revealed the presence of both α-MnOOH and the corundum form of Mn_2O_3 (Fig. 8b). It is therefore proposed that the rapid water loss at low temperatures without equivalent replacement of oxygen from the gas phase leads to an anion-deficient structure in which corundum-phase Mn_2O_3 nucleates, and that this does not lead to the development of a β-MnO_2 structure until the temperature reaches about 350°C (Fig. 8c). This endorses the decomposition path invoked by Lima-de-Faria and Lopes-Vieira (*16*), who also proposed that the formation of corundum-phase Mn_2O_3 takes place during the reaction of α-MnOOH to β-MnO_2.

We conclude that there is no evidence as yet that γ-MnOOH decomposes to β-MnO_2 through a phase of Mn_2O_3 as intermediate. Where this has been suggested, it seems likely that α-MnOOH may have been present as an impurity.

Acknowledgments

The authors wish to thank the Directors of the Berec Group Ltd. for permission to publish this paper and Dr. R. Giovanoli of the University of Bèrne for preparation of a sample of Mn_5O_8.

References

1. M. P. DUBOIS, *Ann. Chim.* **5**, 411 (1936).
2. E. J. W. VERWEY AND J. H. DE BOER, *Rec. Trav. Chim. Pays-Bas* **55**, 531 (1936).
3. W. FEITKNECHT AND W. MARTI, *Helv. Chim. Acta* **28**, 129, 149 (1945).
4. (a) P. BRUNNER, Dissertation, University of Bern (1962); (b) W. FEITKNECHT, *Pure Appl. Chem.* **9**, 423 (1964).
5. H. R. OSWALD, W. FEITKNECHT, AND M. J. WAMPETICH, *Nature* **207**, 72 (1965).
6. H. R. OSWALD AND M. J. WAMPETICH, *Helv. Chim. Acta* **50**, 2023 (1967).
7. M. SATO, K. MATSUKI, M. SUGAWARA, AND T. ENDO, *Nippon Kagaku Kaishi* **9**, 1655 (1973).
8. R. GIOVANOLI AND U. LEUENBERGER, *Helv. Chim. Acta* **52**, 2333 (1969).
9. ASTM, X-Ray Powder Diffraction File 12–733.
10. J. A. LEE, C. E. NEWNHAM, AND F. L. TYE, *J. Colloid Interface Sci.* **42**, 372 (1973).
11. K. J. VETTER AND N. JAEGER, *Electrochim. Acta* **11**, 401 (1966).
12. D. S. FREEMAN AND W. G. CHAPMAN, *Analyst* **96**, 865 (1971).
13. T. E. MOORE, M. ELLIS, AND P. W. SELWOOD, *J. Amer. Chem. Soc.* **72**, 856 (1950).
14. C. DROTSCHMANN, *Batterien* **18**, 686 (1964).
15. A. AGOPSOWICZ, J. L. HITCHCOCK, AND F. L. TYE, *Thermochimica Acta* **32**, 63 (1979).
16. J. LIMA-DE-FARIA AND A. LOPES-VIEIRA, *Mineral. Mag.* **33**, 1024 (1964).
17. ASTM, X-Ray Powder Diffraction File 10–173.
18. ASTM, X-Ray Powder Diffraction File 13–534.
19. C. W. BUNN, *in* "X-Ray Diffraction by Polycrystalline Materials" (H. S. PEISER, H. P. ROOKSBY, AND A. J. C. WILSON, Eds.), p. 344, Institute of Physics (1955).
20. (a) O. BRICKER, *Amer. Mineral.* **50**, 170 (1965); (b) ASTM, X-Ray Powder Diffraction File 18–805.
21. G. GATTOW, *Batterien* **16**, 322 (1962).